

Reflective Display Associated with In-Plane Rotation of Nematic Liquid Crystal

Seung Hee LEE^{1,*}, Seung Ho HONG, Hyang Yul KIM, Dae-Shik SEO², Gi-Dong LEE³ and Tae-Hoon YOON³

TFT Cell Process Development Team, LCD SBU, Hynix Semiconductor Incorporation, San 136-1, Ami-ri, Bubal-eup, Ichon-si, Kyungki-do 467-701, Korea

¹Department of Polymer Science and Technology, Chonbuk National University, Duckjim-dong 664-14, Chonju, Chonbuk 561-756, Korea

²Department of Electrical Computer Engineering, Yonsei University, 134 Shinchon-dong, Seodaemun-ku, Seoul 120-749, Korea

³Department of Electronics Engineering, Pusan National University, Pusan 609-735, Korea

(Received February 13, 2001; accepted for publication May 24, 2001)

We have fabricated a novel reflective nematic liquid-crystal cell driven by a fringe field. In the absence of an electric field, the liquid-crystal molecule is homogeneously aligned and when a fringe field induced by interdigital electrodes is applied, liquid-crystal molecules rotate in plane in the entire whole area. A conventional in-plane switching (IPS) cell was impossible for application to a reflective system due to its low aperture ratio. However, a newly designed fringe-field switching (FFS) cell is possible due to its high transmittance. Furthermore it exhibits a wide viewing angle intrinsically owing to the in-plane rotation of the liquid-crystal director. Several reflective systems with either two polarizers or one polarizer with a quarter-wave retardation film are possible. In this study, we investigate the switching principle of each system and compare their electrooptic characteristics by simulation and experiment.

KEYWORDS: reflective nematic liquid-crystal cell, fringe-field switching, in-plane rotation

1. Introduction

The role of reflective liquid-crystal displays (R-LCDs) is becoming important because they are considered to be suitable devices for mobile information tools (MITs).^{1,2} Recently, several approaches, such as reflective-twisted nematic (R-TN),^{3–5} reflective-optimally compensated bend (R-OCB),⁶ and stacked guest-host display,⁷ have been introduced. However, in order for R-TN and R-OCB to exhibit high image quality, the addition and optimization of optical compensation films are necessary. The transmissive-type display, in-plane switching (IPS), has a wide viewing angle intrinsically owing to the in-plane rotation of the LC director.⁸ However, it has problems such as low light transmittance. Recently, we have developed the “fringe-field switching (FFS)” mode to solve the low transmittance problem, i.e., it can now exhibit both wide viewing angle and high transmittance.^{9–13}

Taking advantage of the in-plane rotation of the LC director that allows realization of a wide viewing angle intrinsically, we apply the FFS mode to the reflective system. There are several ways of designing reflective FFS displays. In this study, we investigate the switching principle and discuss the merits and demerits of the reflective FFS display in different systems by simulation and experiment.

2. Experimental and Simulation Results

To fabricate a cell of the FFS mode, an indium-tin oxide (ITO) layer with a thickness of 400 Å was deposited on the bottom glass substrate and then a passivation layer, SiO₂, with a thickness of 1500 Å was coated by chemical vapor deposition. Finally, a second ITO layer with a thickness of 400 Å was deposited and patterned as interdigital electrodes, as shown in Fig. 1. The width (*w*) of the second ITO electrode was 3 μm and the distance (*l*) between electrodes was 5 μm. There was no electrode on the top glass substrate. An alignment layer (Japan Synthetic Rubber Co., AL-1051) was coated on both substrates and rubbing was carried out in antiparallel directions. The rubbing direction (α) was 78°, which is in the optimal range for maximum trans-

mission.¹⁴ The pretilt angle generated by rubbing was 2°. Two glass substrates were then assembled to realize a cell gap of 4.0 μm. Liquid crystal with negative dielectric anisotropy ($\Delta n = 0.074$ at $\lambda = 589$ nm, $\Delta\epsilon = -3.8$) from Merck Co. was used.

For electrooptic measurement, a Halogen lamp was used as the light source and a square wave, a 60-Hz-voltage source from a function generator was applied to the sample cell. The light reflected from the cell was detected to the photomultiplier tube. For LCDs using the FFS mode, three different types are considered in this study. The first is one with two polarizers. In this case, normally white (NW) and normally black (NB) modes can be achieved. Figure 2 shows the cell

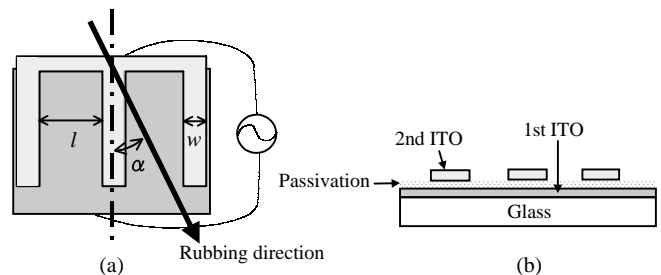


Fig. 1. Top and side views of the electrodes in bottom substrate.

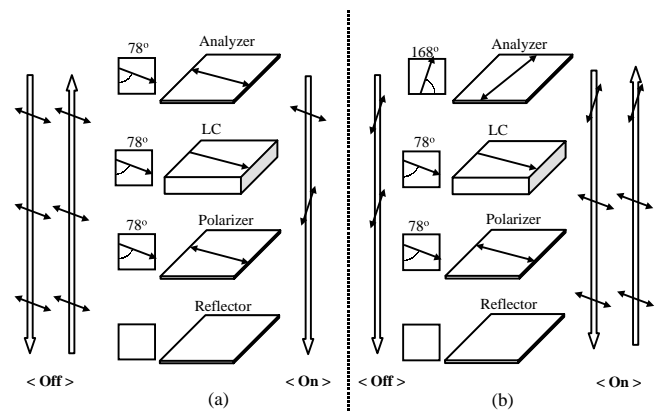


Fig. 2. Configuration of the reflective FFS modes and light passage using two polarizers for (a) NW mode and (b) NB mode.

*E-mail address: lsh1@hynix.com

configurations of both modes with a reflector under the bottom glass substrate. For calculation, the transmittances for the single and parallel polarizers were assumed to be 41% and 36%, respectively. In the NW mode, the rubbing direction is coincident with the transmission axis of the polarizer on the top plate. Then, the transmission axis of the analyzer on the upper plate is parallel to the polarizer on the lower plate. Therefore, when voltage is not applied, linearly polarized incident light passing through the analyzer in the normal direction is reflected without any loss of light intensity except for that absorbed by the polarizers. As voltage is applied to rotate the LC director by 45°, the polarization of the incident light is rotated by 90° through the LC layer, and the polarizer absorbs the light so that the cell appears black. In the NB mode, the axis of the analyzer is orthogonal to the polarizer. As a result, the polarizer blocks the linearly polarized light that passes through the LC layers and the cell appears black. When voltage is applied, the optical axis of the LC director deviates from that of the analyzer and the linearly polarized light becomes elliptic such that some of the light passes through the polarizer and is reflected by the reflector.

The electrooptic characteristics of the reflective FFS cell are simulated based on the 2×2 extended Johns method to simulate the voltage-dependent reflectivity in normal direction and the viewing angle characteristics.¹⁵⁾ The retardation value of the cell is $0.3 \mu\text{m}$, which is effective to the half-wavelength. Figure 3 shows voltage-dependent reflectivity curves for both modes. The reflectivity of the NW cell is 28.6%, which is slightly better than that of the NB cell (22.9%), where the reflectivity of a single polarizer on the reflector is assumed to be 36%. However, the dark state of the NB cell is better than that of the NW cell. The calculated contrast ratios for NW and NB cells are 105 and greater than 1000, respectively. That is, the NW cell is favored for brightness, while the NB cell, for contrast ratio. For both cells, the operating voltage is about 5 V, which is slightly higher than that of the R-TN mode,⁴⁾ because in the reflective FFS

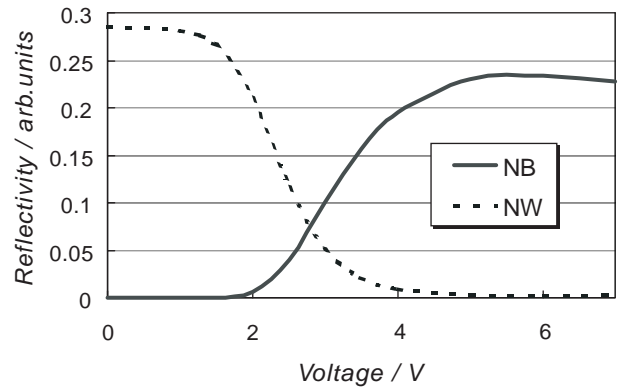


Fig. 3. Calculated voltage-dependent reflectivity curves in the NB and the NW modes.

cell, light undergoes a full change in birefringence before it is reflected. The viewing angle characteristics of NW and NB cells for five grey levels are calculated in the horizontal direction, and the results are shown in Fig. 4. Grey scale inversion does not occur even at a polar angle of 70°. These results prove that the reflective FFS cell exhibits wide viewing angle characteristics.

Another reflective system, the NB mode, uses a quarter-wave retardation film with a single polarizer. Figure 5 shows the cell structure and switching principle of the device. In the off state, the linearly polarized light that passes through the analyzer maintains its state of polarization as it propagates through the cell because the optical axis of the LC director is coincident with that of the analyzer. However, the slow axis of the retardation film below the cell makes an angle of 45° with respect to the analyzer, so that the linearly polarized light becomes circularly polarized light. Here, the retardation film is assumed to be a quarter-wave plate through the entire visible wavelength region. Now, the reflected circularly polarized light becomes linearly polarized after passing

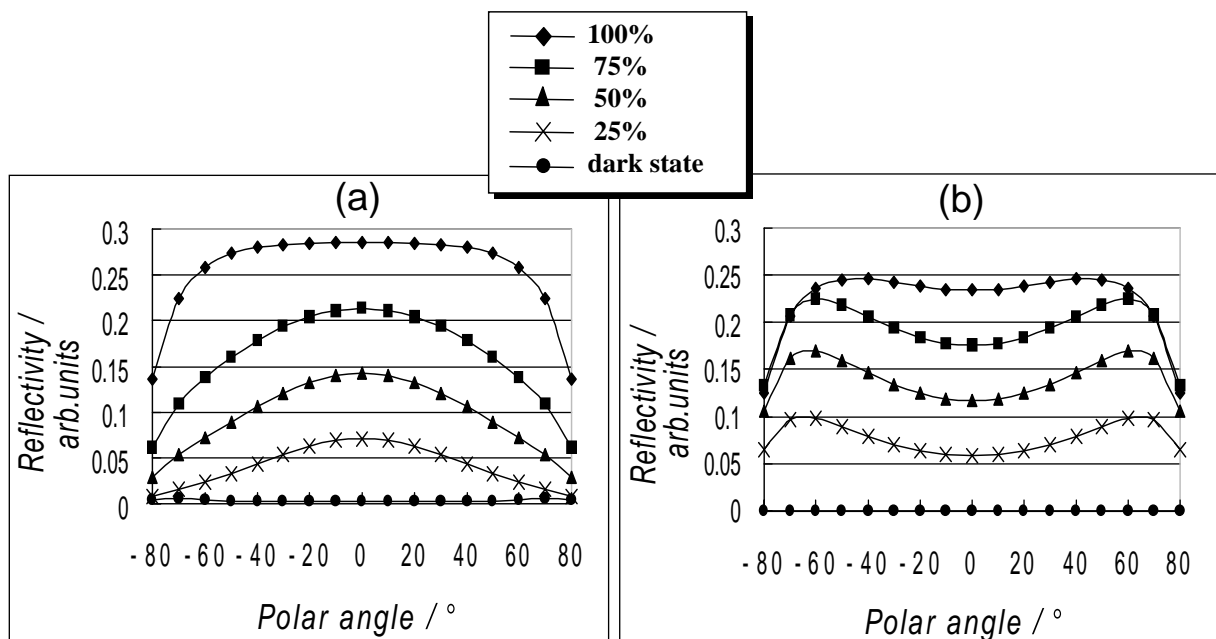


Fig. 4. Calculated viewing angle characteristics in horizontal direction using two polarizers for (a) NW mode and (b) NW mode, where % indicates relative reflectance at normal direction.

through the retardation film, because the quarter-wave plate transforms the circularly polarized light into the linearly polarized light. However, this linearly polarized light is rotated by 90° compared with the incident light. Finally, the analyzer

blocks the linearly polarized light so that the dark state is realized. Therefore, in the off state, we need not consider the retardation of the cell for perfect dark state. For the bright state of the cell with a half-wave retardation, the optic axis of the half-wave LC layer is rotated by 22.5° by applying an appropriate voltage to the cell. Then, the linearly polarized input light is rotated by 45° by passing through the LC layer. Now, the polarization is parallel to the optical axis of the quarter-wave retardation film. Therefore, the light maintains the polarization during the double passage through the quarter-wave film. Then, the reflected light is rotated by -45° by propagating through the LC layer once more. Finally, the reflected light is linearly polarized again, which is parallel to the transmission axis of the polarizer. Thus, the bright state is realized. Figure 6 shows the calculated results for driving voltage and reflectivity as function of the retardation value of the liquid crystal, where the cell gap is fixed at 4 μm. The data show that the maximum reflectivity (R_{max}) of the device has been realized at the retardation value of 0.2 μm and the operation voltage (V_{max}) is peaked at the retardation value 0.2 μm, and rapidly decreases as the retardation value increases further. From these results, we have chosen the retardation of the cell to be 0.3 μm. Figure 7 shows the simulated viewing angle characteristics. In the horizontal and vertical directions, grey scale inversion of more than 100° occurs and the calculated reflectivity is 31.4%, which is relatively high compared with that of the cells with two polarizers. Moreover, the operation voltage is about one-half that of the cells with two polarizers because the degree of rotation of the LC director is about half that of those with two polarizers. Figure 8 shows the measured voltage-dependent transmittance curve of the cell where the light source is located at a polar angle of -30° and is detected at a polar angle of 10°. The voltage showing maximum transmittance is 3.5 V, which is lower than those of previous cases although the dielectric anisotropy of the LC is only -3.8. In conclusion, the device has such advantages as high reflectance, wide viewing angle and low driving voltage. In addition, the NW mode of the device is also possible even if the LC optical axis deviates by 22.5° of from the polarizer. An alternative reflective system is that with a single

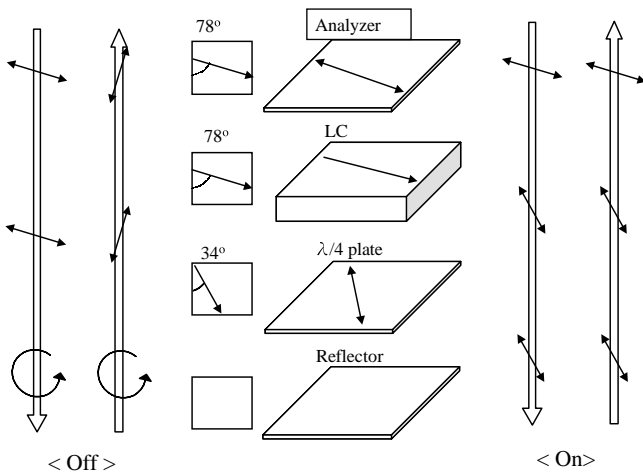


Fig. 5. Cell structure and light passage using one polarizer with quarter-wave plate.

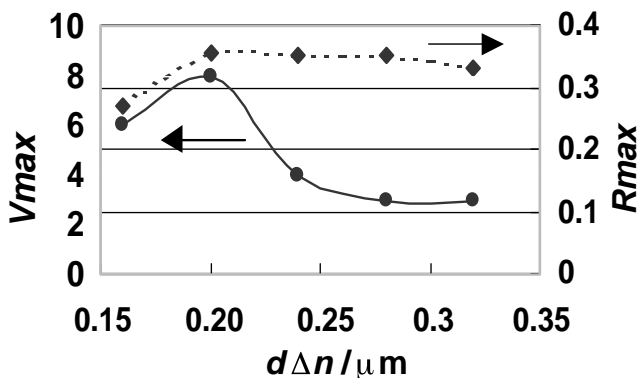


Fig. 6. Maximum reflectivity and operation voltage as a function of the retardation of the liquid crystal layer using one polarizer with quarter wave plate.

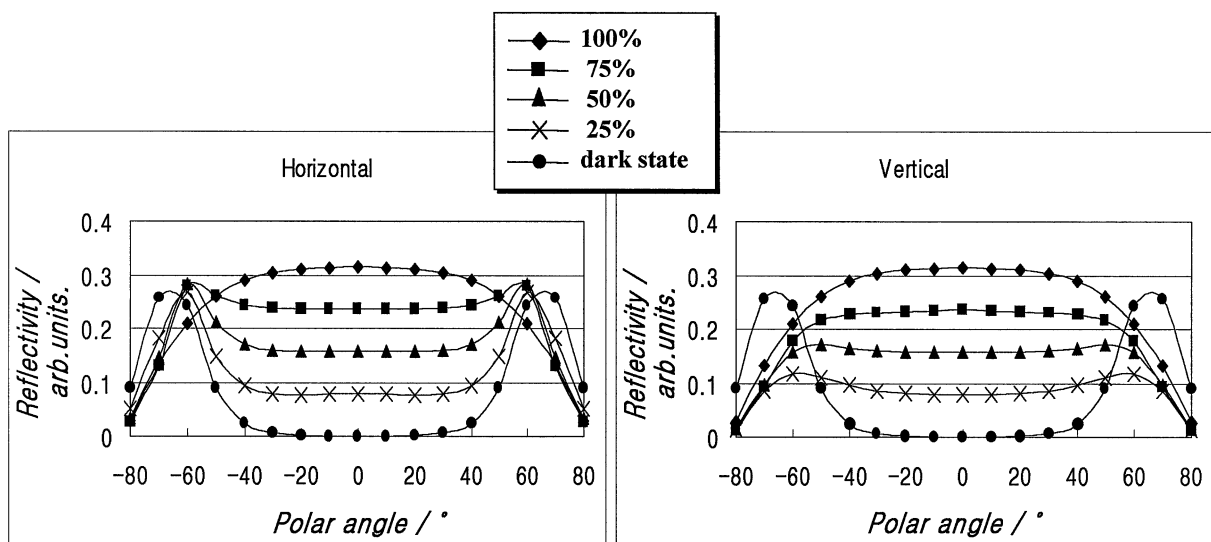


Fig. 7. Simulated results of the viewing angle characteristics using the one polarizer with quarter-wave plate.

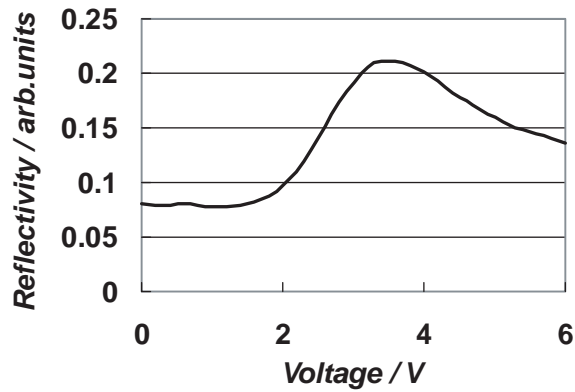


Fig. 8. Voltage-dependent reflectivity curve using one polarizer with quarter-wave plate.

polarizer and a cell retardation value of $(n/2 + 1/4)\lambda$ where n is 0, 1, 2, However, the fabrication of a cell with a retardation of $\lambda/4$ is rather difficult because of the low cell gap.

3. Conclusions

In summary, we proposed another reflective display using the FFS mode. Due to in-plane orientation of the LC director, the device has a wide viewing angle without occurrence

of grey scale inversion over a wide range of viewing angle, irrespective of the number of polarizers. In particular, the device with one polarizer and quarter-wave plate has low driving voltage, which is advantageous in terms of low power consumption.

- 1) T. Uchida, T. Nakayama, T. Miyashita, M. Suzuki and T. Ishinabe: IDRC Dig., 1995, p. 599.
- 2) T. Ogawa, S. Fujita, Y. Iwai and H. Koseki: SID Dig., 1998, p. 217.
- 3) Y. Itoh, S. Fujiwara, N. Kimuta, S. Mizushima, F. Funada and M. Hijikigawa: SID Dig., 1998, p. 221.
- 4) Y. Iwai, H. Yamaguichi, T. Sekime, H. Kinoshita, S. Fujita, H. Mizuno, T. Hatanaka, T. Ohtani and T. Ogawa: SID Dig., 1998, p. 225.
- 5) M. Shibazaki, T. Ishinabe, T. Miyashita, T. Uchida, K. Yoshida, H. Tanaka and T. Sunata: SID Dig., 1999, p. 690.
- 6) T. Ishinabe, T. Miyashita and T. Uchida: SID Dig., 1999, p. 698.
- 7) K. Takeda, M. Hasegawa, Y. Sakaguchi, Y. Taira, J. Egelhaaf, E. Lueder and A. C. Lowe: SID Dig., 1999, p. 702.
- 8) M. Ohta, M. Oh-e and K. Kondo: IDRC Dig., 1995, p. 707.
- 9) S. H. Lee, S. L. Lee and H. Y. Kim: Appl. Phys. Lett. **73** (1998) 2881.
- 10) S. H. Lee, S. L. Lee and H. Y. Kim: IDRC Dig., 1998, p. 371.
- 11) S. H. Lee, S. L. Lee, H. Y. Kim and T. Y. Eom: SID Dig., 1999, p. 202.
- 12) S. H. Lee, H. Y. Kim and S. L. Lee: IDW Dig., 1999, p. 191.
- 13) S. H. Lee, S. L. Lee, H. Y. Kim and T. Y. Eom: J. Kor. Phys. Soc. **35** (1999) S1111.
- 14) S. H. Hong, I. C. Park, H. Y. Kim and S. H. Lee: Jpn. J. Appl. Phys. **39** (2000) L527.
- 15) A. Lien: Appl. Phys. Lett. **57** (1990) 2767.